Lecture Notes Black Holes and Gravitational Waves

Maarten van de Meent

April 2024

Contents

Conventions

We will be using the following conventions through out these notes.

- We work in geometric units such that $G = c = 1$.
- We utilize **abstract index notation** to refer to tensors. This means that abstract tensors are always denoted with indices that indicate the type and rank of the tensor. This does not signify that any particular coordinate basis has been chosen. Repeated indices of opposite type will denote contractions.

Chapter 1

Penrose Diagrams

Literature:

- Reall, Chap. 5
- Carroll, Sec. 5.6, 5.7 and Appendix H

In this chapter we will develop the tools to describe the causal structure of a spacetime, allowing us to define what it means for a spacetime to contain a black hole.

1.1 Conformal transformations

Given a metric $g_{\mu\nu}$ on a spacetime M, we can define a new metric $\bar{g}_{\mu\nu}$ as $\bar{g}_{\mu\nu} = \omega(x)^2 g_{\mu\nu}$, where $\omega : M \to \mathbb{R}$ is a positive smooth function. This new metric $\bar{g}_{\mu\nu}$ in general defines a new spacetime geometry. Nonetheless, this new geometry will agree with the old geometry on the notions of curves being "timelike", "spacelike", or "null", i.e. they will agree on the possible causal relations between different spacetime events; the **causal structure** of the spacetime. The transformation from $g_{\mu\nu}$ to $\bar{g}_{\mu\nu}$ encoded by the function $\omega(x)$ is known as a **conformal transformation**, since it preserves the angles (but not lengths) of the geometry.

The idea is to use these conformal transformations to take a (generally infinite) spacetime and map it to a compact spacetime (which we can draw on a page) with the same causal structure.

1.2 Minkowski space

We start with the Minkowski space. In spherical coordinates the Minkowski metric reads

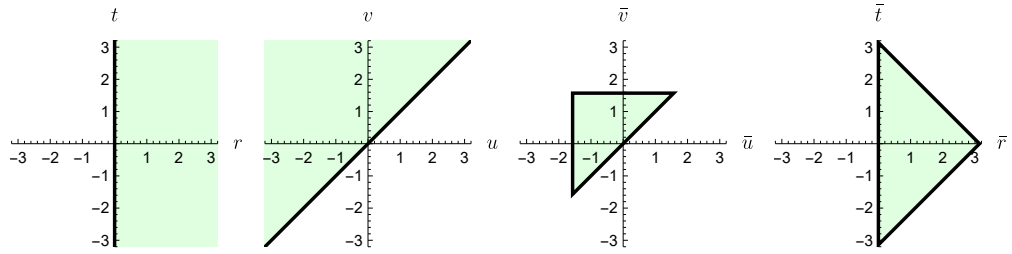

Figure 1.1: Illustration of the ranges of the different coordinates used in this section.

$$\eta_{\mu\nu} = -dt^2 + dr^2 + r^2(d\theta^2 + \sin^2\theta d\phi^2), \tag{1.1}$$

with the coordinate ranges (which will become important later on) $t \in (-\infty, \infty)$, $r \in [0, \infty)$, $\theta \in [0, \pi]$, and $\phi \in [-\pi, \pi]$. Our first step is to define lightcone coordinates

$$u = t - r, \qquad \text{and} \qquad v = t + r, \tag{1.2}$$

which gives the metric

$$\eta_{\mu\nu} = -dudv + \frac{1}{4}(v-u)^2(d\theta^2 + \sin^2\theta d\phi^2), \tag{1.3}$$

with ranges $-\infty < u \leq v < \infty$. We can compactify the range of our coordinates by choosing new coordinates $(\bar{u}, \bar{v})$ defined by,

$$u = \tan\bar{u}, \qquad \text{and} \qquad v = \tan\bar{v}, \tag{1.4}$$

which reduces the ranges to $-\pi/2 < \bar{u} \leq \bar{v} < \pi/2$, and gives the metric

$$\eta_{\mu\nu} = (2\cos\bar{u}\cos\bar{v})^{-2}\left(-4d\bar{u}d\bar{v} + \sin^2(\bar{v}-\bar{u})(d\theta^2 + \sin^2\theta d\phi^2)\right). \tag{1.5}$$

To find the conformal compatification of Minkowski space, we finally define the function

$$\omega = 2\cos\bar{u}\cos\bar{v}, \tag{1.6}$$

and the coordinates

$$\bar{t} = \bar{u} + \bar{v}, \qquad \text{and} \qquad \bar{r} = \bar{v} - \bar{u}, \tag{1.7}$$

to find the metric

$$\bar{\eta}_{\mu\nu} = -d\bar{t}^2 + d\bar{r}^2 + \sin^2\bar{r}(d\theta^2 + \sin^2\theta d\phi^2). \tag{1.8}$$

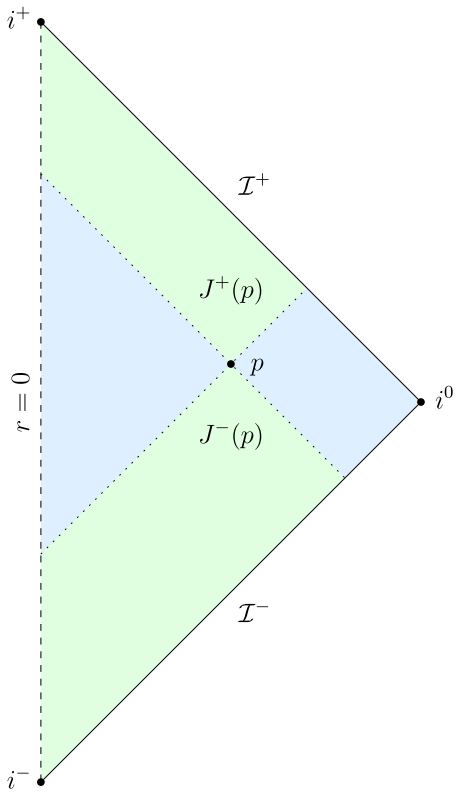

Figure 1.2: The Penrose diagram for Minkowski space.

The astute reader may recognize this as the line element of the Einstein static universe, $\mathbb{R} \times S^3$ (see Harmark Ex. 4.3). However, the crucial difference lies in the range of the coordinates, in particular $0 \leq \bar{r} < \pi$ and $-\pi + \bar{r} < \bar{t} < \pi - \bar{r}$ (see Fig. 1.1). By projecting onto the $(\bar{r}, \bar{t})$-plane, we obtain the **Penrose diagram** for Minkowski space, shown in Fig. 1.2. Each interior point of the shown region represents a 2-sphere in the full spacetime. The dashed boundary at $\bar{r} = 0$ represents the symmetry axis at $r = 0$ of the original coordinates, and the outer boundary denotes the points originally "at infinity".

To understand the structure of "infinity" we can consider the behavior of radial geodesics in the diagram. By construction of the diagram all radial null geodesics travel along 45 degree lines. Any null geodesic will originate at $\mathcal{I}^-$, travel along an inwards 45 degree straight line until it reaches $r = 0$, and reflect back to an outwards 45 degree line until it reaches $\mathcal{I}^+$. We therefore refer to $\mathcal{I}^-$ as **past null infinity**, and $\mathcal{I}^+$ as **future null infinity**. In a similar vein, all radial spacelike geodesics start and end at i^0, which we call

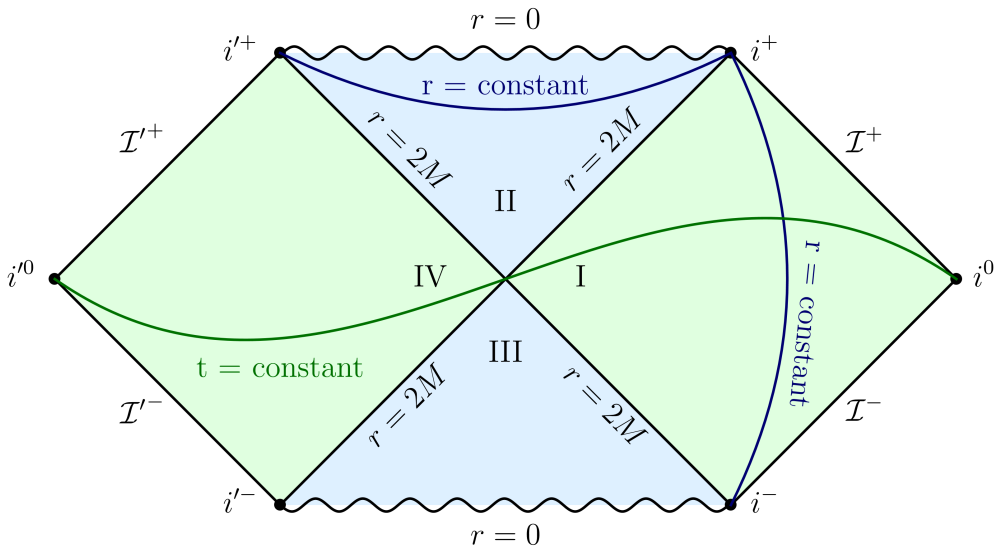

Figure 1.3: The Penrose diagram for the maximally extended Schwarzschild spacetime.

spatial infinity, and timelike geodesics start at i^- and end at i^+, which are called **past** and **future timelike infinity**, respectively.

A spacetime whose Penrose diagram has a structure near infinity resembling[1] that of Minkowski space is called **asymptotically flat**.

Finally, we use the Penrose diagram of Minkowski space to visualize to more important concepts related to the causal structure of spacetime. Given an event $p \in M$, the set of all events that can be connected to p with a future-directed causal (i.e. timelike or null) curve ending in p, is called the **causal past of** p, and denoted J^-. In the Penrose diagram the intersection of $J^-(p)$ with a constant (θ, ϕ)-slice is simply the 45-degree wedge below the point p as shown in Fig. 1.2. Similarly, the set of all events that can be connected to p with a future-directed causal (i.e. timelike or null) curve starting at p, is called the **causal future of** p, and denoted $J^+(p)$.

1.3 Schwarzschild

In the course by Harmark you were introduced to the Schwarzschild metric,

[1]For a more precise technical discussion of what "resembling" means in this context, see Chapter 5 of Reall's lecture notes.

$$g_{\mu\nu} = -(1 - \frac{2M}{r})dt^2 + \frac{dr^2}{1 - \frac{2M}{r}} + r^2(d\theta^2 + \sin^2\theta d\phi^2). \tag{1.9}$$

This metric has a (coordinate) singularity at $r = 2M$. Consequently, the a priori domain of the coordinates is $-\infty < t < \infty$ and $2M < r < \infty$. By changing the time coordinate to (advanced) Eddington-Finkelstein time

$$v = t + r^* \quad \text{with} \quad r^* = r + 2M \log\left(\frac{r - 2M}{2M}\right), \tag{1.10}$$

you were shown that the validity of the Schwarzschild metric can be extended to $0 < r < \infty$ for infalling observers. The same reasoning can be applied when using the retarded Eddington-Finkelstein time coordinate $u = t - r^*$ to shown that there exists an (inequivalent) extension of Schwarzschild to for the past of outgoing observers. When using both u and v to form double null coordinates we obtain

$$g_{\mu\nu} = -\left(1 - \frac{2M}{r(u,v)}\right) du dv + r(u,v)^2(d\theta^2 + \sin^2\theta d\phi^2). \tag{1.11}$$

Even with the maximal coordinate range $-\infty < u, v < \infty$ these coordinates correspond only to the $2M < r < \infty$ Schwarzschild patch. The $r = 2M$ boundary corresponds to the $u \to \infty$ and $v \to -\infty$ limits. To find coordinates that cover all of the extended spacetime we introduce rescaled null coordinates

$$u = -4M \log(-\underline{u}) \quad \text{and} \quad v = 4M \log(\underline{v}). \tag{1.12}$$

In these coordinates the original Schwarzschild patch is covered by $-\infty < \underline{u} < 0$ and $0 < \underline{v} < \infty$. With these coordinates the Schwarzschild metric takes its **Kruskal-Szekeres** form,

$$g_{\mu\nu} = -\frac{32M}{r(\underline{u},\underline{v})} e^{-\frac{r}{2M}} d\underline{u} d\underline{v} + r(\underline{u},\underline{v})^2(d\theta^2 + \sin^2\theta d\phi^2), \tag{1.13}$$

where r is defined implicitly through the relation $\underline{u}\,\underline{v} = (r/(2M) - 1)e^{r/(2M)}$. This form is manifestly smooth at $\underline{u} = 0$ and $\underline{v} = 0$ (i.e. $r = 2M$), and be extended beyond this point.

To produce the Penrose diagram we can again compactify the range of $\underline{u}$ and $\underline{v}$ by introducing

$$\underline{u} = \tan\bar{u}, \qquad \text{and} \qquad \underline{v} = \tan\bar{v}, \tag{1.14}$$

and an appropriate conformal factor ω such that we obtain a compactified metric of the form

$$\bar{g}_{\mu\nu} = -2d\bar{u}d\bar{v} + R(\bar{u},\bar{v})^2(d\theta^2 + \sin^2\theta d\phi^2). \tag{1.15}$$

(the explicit form of ω and R is messy and not particularly illuminating).

The resulting Penrose diagram is shown in Fig. 1.3. The original Schwarzschild patch (marked "I") is asymptotically flat. The original (advanced) Eddington-Finkelstein coordinates extend the metric to region "II" allowing objects to fall into the black hole and reach the singularity at $r = 0$. The corresponding construction with the retarded time extends the metric to region "III", allowing the worldline to extend to the singularity in their past.

Finally, we are presented with a second asymptotically flat region ("IV"), complete with its own copies of future and past null infinity ($\mathcal{I}'^+$ and $\mathcal{I}'^-$), future and past timelike infinity (i'^+ and i'^-), and spacelike infinity i'^0. There are no causal curves that connect regions I and IV. So, for an observer in region I, region IV might as well not exist, and vice versa. There are however spacelike curves that connect regions I and IV. This "worm hole" between "parallel universes" is known as an **Einstein-Rosen bridge**. Because it consists solely of spacelike curves, there is no way to transverse it.

1.3.1 Definition of a Black Hole

We are now ready to give a precise definition of a black hole:

Definition 1. Let $(M, g_{\mu\nu})$ be a spacetime that is asymptotically flat at null infinity. The **black hole region** is $\mathcal{B} = M \setminus J^-(\mathcal{I}^+)$. The boundary of $\mathcal{B}$, $\partial\mathcal{B}$ is called the **future event horizon**, $\mathcal{H}^+$. Similarly, $\mathcal{W} = M \setminus J^+(\mathcal{I}^-)$ is the **white hole region**, and its boundary $\partial\mathcal{W}$, the **past event horizon**, $\mathcal{H}^-$.

In more plain English a black hole consists of those events in spacetime from which no signal can reach future null infinity, a white hole consists of those events which cannot be reached by any signal starting at past null infinity. A direct consequence of this definition is that an event horizon is always a null-surface.

Concretely, when we look at the Penrose diagram for Schwarzschild in Fig. 1.3, we see that the black hole region $\mathcal{B}$ corresponding to $\mathcal{I}^+$ consists of the union of regions II and IV, and the future event horizon $\mathcal{H}^+$ is the boundary $\bar{u} = 0$, where $r = 2M$. The white hole region $\mathcal{W}$ is the union of regions III and IV, and the past event horizon is $\mathcal{H}^-$ is the boundary $\bar{v} = 0$, where $r = 2M$ as well.

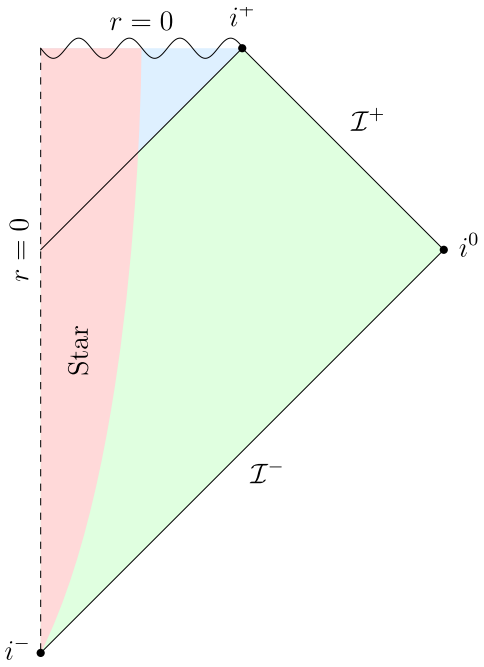

Figure 1.4: The Penrose diagram for a spherically symmetric star collapsing to a black hole.

Note that since the maximally extended Schwarzschild spacetime has two asymptotically flat regions, each region has its own black (white) hole regions. Relative to $\mathcal{I}'^+$ the black hole consists of the unions of I and II, and relative to $\mathcal{I}'^-$ the white hole consists of regions I and III.

1.3.2 Spherical collapse

The maximally extended Schwarzschild solution contains some fantastical features (wormholes, parallel universes, etc.). A good question to ask ourselves is which of these features arise from the strict symmetry constraints (vacuum, spherical symmetry, static), and which features survive in a more realistic scenario. To this end we display the Penrose diagram for a spherically symmetric star collapsing to a black hole in Fig. 1.4. Outside of the star, the spacetime is spherically symmetric and vacuum, and therefore — by Birkhoff's theorem — given by the Schwarzschild solution. The interior of the star, which encapsulates $r = 0$ at early times, is given by a more regular solution.

We see that the only fantastical feature that remain is the formation of an event horizon, black hole region, and singularity. All the more science

fiction sounding features like white holes, worm holes, and parallel universes have disappeared due to the inclusion of a matter distribution.

1.4 The Kerr Black Hole

The Kerr solution for a rotating black hole was introduced in Sec. 3.3 of Harmark's notes. In Boyer-Lindquist coordinates it is given by

$$g_{\mu\nu} = -\left(1 - \frac{2Mr}{\Sigma}\right) dt^2 - \frac{4Mar}{\Sigma} \sin^2\theta dt d\phi + \frac{(r^2+a^2)^2 - a^2\Delta \sin^2\theta}{\Sigma} \sin^2\theta d\phi^2 + \frac{\Sigma}{\Delta} dr^2 + \Sigma d\theta^2, \tag{1.16}$$

with

$$\Sigma(r,\theta) = r^2 + a^2\cos^2\theta, \quad \text{and} \tag{1.17}$$

$$\Delta(r) = r^2 - 2Mr + a^2 = (r - r_+)(r - r_-). \tag{1.18}$$

This metric has a trivial coordinate singularity at $\theta = 0$ and $\theta = \pi$, coordinate singularities at $r = r_\pm = M \pm \sqrt{M^2 - a^2}$ corresponding to horizons, and a true curvature ring singularity at $r = 0$ and $\theta = \pi/2$.

The coordinate singularities at $r = r_\pm$ divide the metric in three disjoint patches ($r_+ < r < \infty$, $r_- < r < r_+$, and $-\infty < r < r_-$) that, a priori, are unrelated. The different patches can be related to each other using a similar procedure as in Schwarzschild using advanced and retarded time coordinates. We will not discuss the details here[2], instead we simply present the resulting Penrose diagram in Fig. 1.5.

From region I we can again traverse into a black hole by crossing $r = r_+$ into region II. In region II the r direction is timelike and we can only proceed to smaller values of r until we cross $r = r_-$ into region V (or V'). In region the r-direction is again spacelike and worldlines can both proceed to smaller r or (as will be the case for almost all geodesics) back outward to larger r until we cross $r = r_-$ again and enter region III'. Here r is again timelike and we can only proceed further outward until we cross $r = r_+$ into region I', a new distinct copy of region I (or its parallel universe region IV'). From here we can continue ad infinitum to find an infinity stack of new asymptotically flat regions.

In region V we could have also proceeded to $r = 0$. Only for $\theta = \pi/2$ is this a singularity. For all other values of θ we are free to cross into the $r < 0$

[2]For the full details see [2]

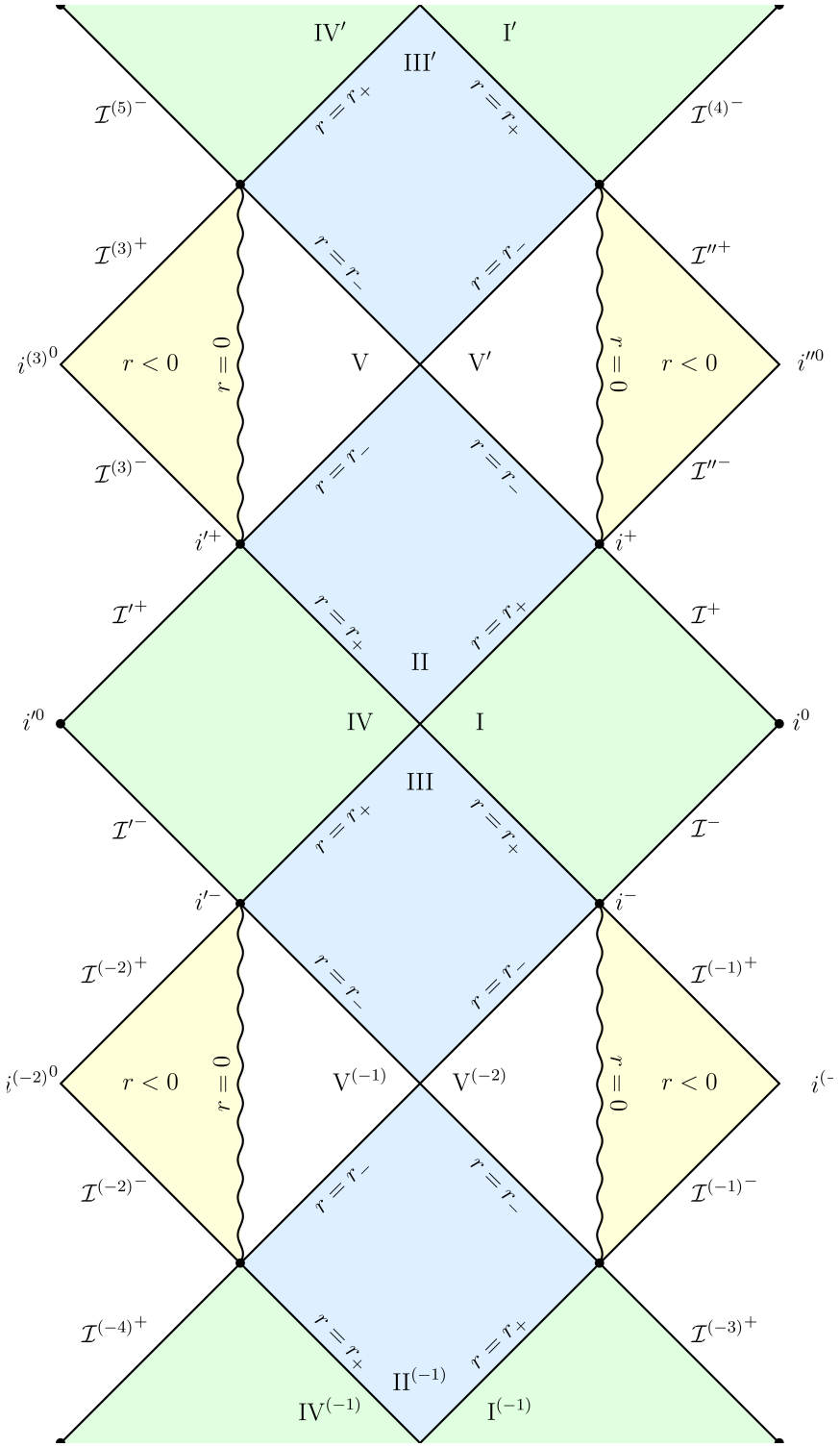

Figure 1.5: The Penrose diagram for a maximally extended Kerr black hole.

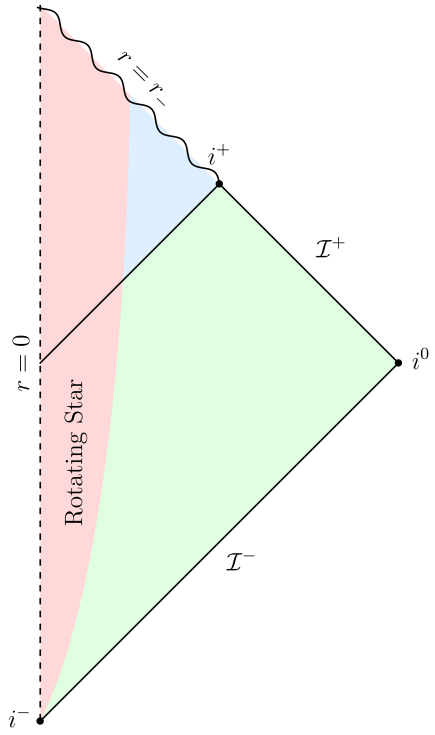

Figure 1.6: A sketch of the Penrose diagram for a rotating star collapsing to a Kerr black hole.

region. This region is again asymptotically flat but now in the $r \to -\infty$ limit. However, in this region there is no horizon to shield future null infinity from the singularity at $r = 0$, the singularity is **naked**. To make matters worse, this region also has closed timelike curves, breaking causality.

1.4.1 Collapse of a rotating black hole

Maximally extended Kerr is even more fantastical than its non-rotating counter part. It is therefore a good idea to regain our grounding and look at a more realistic collapse scenario. Unfortunately, there is no equivalent of Birkhoff's theorem for rotating geometries. Consequently, we are not guaranteed that the spacetime outside of the star is exactly Kerr. Instead we have to make do with the much weaker result from the no hair theorem that after the collapse the region outside the horizon has to settle down to a member of the Kerr(-Newman) family.

Most of the really fantastical features of maximally extended Kerr man-

ifest themselves after crossing the $r = r_-$ boundary. How much should we really trust the solution after this point. The first thing to note is that this boundary is a **Cauchy horizon**, meaning that if we try to construct the solution for initial data on some timelike slice this is the absolute limit we can evolve or solutions before singularities start to appear somewhere in our domain of dependence. We should be very wary of the analytically extended version of the solution beyond this point, because it cannot be obtained through a natural evolution. Second, we note that if we take an event on the Cauchy horizon between region II and V' its causal history $J^-(p)$ will actual contain all of region I (for some value of θ). An observer crossing this line is therefore confronted with an infinity amount of history in a finite amount of time. Consequently, even the tiniest perturbation of the spacetime is likely to be blue shifted to something singular. It is therefore conjectured that this Cauchy surface will become singular for generic perturbations away from Kerr.

Based on these conjectures we sketch what the Penrose diagram for a rotating collapsing star likely looks like in Fig. 1.6. The final result looks remarkably like the Schwarzschild case, avoiding the most fantastical behaviour of the maximally extended Kerr.

Chapter 2

Geodesics in Kerr Spacetime

2.1 The geodesic equation

Literature: Harmark, Sec. 1.3.3 and 1.4.6; Carroll Sec. 3.3 and 3.4

In the first GR course you saw the geodesic equation

$$\frac{D}{ds}\frac{\mathrm{d}x^\mu}{\mathrm{d}s} = \frac{\mathrm{d}x^\alpha}{\mathrm{d}s}\nabla_\alpha\frac{\mathrm{d}x^\mu}{\mathrm{d}s} = \frac{\mathrm{d}^2x^\mu}{\mathrm{d}s^2} + \Gamma^\mu_{\alpha\beta}\frac{\mathrm{d}x^\alpha}{\mathrm{d}s}\frac{\mathrm{d}x^\beta}{\mathrm{d}s} = 0. \tag{2.1}$$

Solving this equation can be made easier by first identifying constants of motion, the existence of which is intertwined with the notion of spacetime symmetries.

2.2 Symmetries and Killing vectors

Literature: Carroll Sec. 3.8 and Appendix B, Wald Appendix C

A symmetry of a spacetime M is a automorphism $\phi : M \to M$ that leaves the spacetime "invariant". Infinitesimal automorphisms are given by vector fields in the following way. Suppose we have a (smooth) vector field V^μ, we can construct a family of automorphisms $\phi^t_{V^\mu}$ indexed by a variable $t \in \mathbb{R}$ by mapping each event $p \in M$ to a new event p' by following the integral curves of V^μ for a time t. (I.e. we solve the differential equation $\frac{\mathrm{d}x^\mu}{\mathrm{d}t} = V^\mu$ with initial condition $x(0) = p$, and set $p' = x(t)$.)

We can try to ask ourselves the question how does a $T_{\mu_1\ldots\mu_n}$ change along the integral lines of V^μ. Naively one may try to write the down the derivative

$$\lim_{t\to 0}\frac{T_{\mu_1\ldots\mu_n}(p') - T_{\mu_1\ldots\mu_n}(p)}{t}.$$

However, such an expression does not make any mathematical sense. The tensors $T_{\mu_1\ldots\mu_n}(p')$ and $T_{\mu_1\ldots\mu_n}(p)$ belong to (the tensor product of) the

(co)tangent space at different points in M. Consequently, we cannot add (or subtract) them. To get another object that lives at p, we can consider the map induced by $\phi^t_{V^\mu}$ on the tensor bundles (the push forward), or more specifically its inverse (the pull back) $(\phi^t_{V^\nu})^*$, which in terms of components is given by

$$\left(\left(\phi^t_{V^\nu}\right)^* T\right)_{\mu_1\ldots\mu_n}(p) = \frac{\partial p'^{\alpha_1}}{\partial p^{\mu_1}} \cdots \frac{\partial p'^{\alpha_n}}{\partial p^{\mu_n}} T_{\alpha_1\ldots\alpha_n}(p').$$

This allows us to define a derivative that is defined covariantly and expresses how much a tensor field changes in the direction of a vector field V^μ.

Definition 2. Given a vector field V^μ and a tensor field $T_{\mu_1\ldots\mu_n}$ we can define the **Lie**[1] **derivative** of $T_{\mu_1\ldots\mu_n}$ w.r.t. V^μ at an event p as follows,

$$\mathcal{L}_{V^\nu} T_{\mu_1\ldots\mu_n}(p) = \lim_{t\to 0} \frac{\left((\phi^t_{V^\nu})^* T_{\mu_1\ldots\mu_n}\right)(p) - T_{\mu_1\ldots\mu_n}(p)}{t}$$

Note that this notion of derivative does not require the existence of a metric. This makes it suitable to explore the symmetries of the metric itself. In particular, if we calculate the Lie derivative of a metric tensor $g_{\mu\nu}$ we find

$$\begin{aligned}
\mathcal{L}_{K^\lambda} g_{\mu\nu} &= \lim_{t\to 0} \frac{\left((\phi^t_{V^\nu})^* g_{\mu\nu}\right)(p) - g_{\mu\nu}(p)}{t} \\
&= \lim_{t\to 0} \frac{\frac{\partial p'^\alpha}{\partial p^\mu}\frac{\partial p'^\beta}{\partial p^\nu} g_{\alpha\beta}(p') - g_{\mu\nu}(p)}{t} \\
&= \lim_{t\to 0} \frac{\left(\delta^\alpha_\mu + t\partial_\mu V^\alpha\right)\left(\delta^\beta_\nu + t\partial_\nu V^\beta\right)\left(g_{\alpha\beta}(p) + tV^\gamma \partial_\gamma g_{\alpha\beta}(p)\right) - g_{\mu\nu}(p)}{t} \\
&= g_{\alpha\nu}\partial_\mu V^\alpha + g_{\mu\beta}\partial_\nu V^\beta + V^\gamma \partial_\gamma g_{\mu\nu} \\
&= \partial_\mu V_\nu - V^\alpha \partial_\mu g_{\alpha\nu} + \partial_\nu V_\mu - V^\beta \partial_\nu g_{\mu\beta} + V^\gamma \partial_\gamma g_{\mu\nu} \\
&= \partial_\mu V_\nu + \partial_\nu V_\mu - V^\alpha \left(\partial_\mu g_{\alpha\nu} + \partial_\nu g_{\mu\alpha} - \partial_\alpha g_{\mu\nu}\right) \\
&= \partial_\mu V_\nu + \partial_\nu V_\mu - 2V_\alpha \Gamma^\alpha_{\mu\nu} \\
&= \nabla_\mu V_\nu + \nabla_\nu V_\mu = 2\nabla_{(\mu} V_{\nu)}.
\end{aligned}$$

We are now ready to introduce the notion of a symmetry of spacetime $(M, g_{\mu\nu})$.

Definition 3. Let K^μ be a vector field on a (pseudo)-Riemannian manifold $(M, g_{\mu\nu})$. K^μ is called a **Killing**[2] vector (field) if equivalently:

[1] Pronounced "Lee" after 19th century Norwegian mathematician Sophus Lie.

[2] After the 19th century German mathematician, Wilhelm Killing.

1. $\mathcal{L}_{K^\lambda} g_{\mu\nu} = 0$
2. $\nabla_{(\mu} K_{\nu)} \equiv \frac{1}{2}(\nabla_\mu K_\nu + \nabla_\nu K_\mu) = 0$

Killing vectors encode the symmetries of a spacetime geometry. Sometimes coordinates make it easy to find Killing vectors, as described by the following lemma.

Lemma 1. *If the components of a metric $g_{\mu\nu}$ in some particular coordinates do not depend on the coordinate k, then $\left(\frac{\partial}{\partial k}\right)^\mu$ is a Killing vector field.*

Proof. Left as an exercise to the reader. □

This leads to the main result that will help us solve the geodesic equation in Kerr.

Lemma 2. *Let $x^\mu(s)$ be a geodesic on a (pseudo)-Riemannian manifold $(M, g_{\mu\nu})$, and let K^μ be a Killing vector field, then the quantity $\mathcal{K} = K_\alpha \frac{\mathrm{d}x^\alpha}{\mathrm{d}s}$ is conserved along the geodesic $x^\mu(s)$.*

Proof.

$$\begin{aligned}
\frac{\mathrm{d}\mathcal{K}}{\mathrm{d}s} &= \frac{\mathrm{d}x^\alpha}{\mathrm{d}s}\nabla_\alpha \mathcal{K} && (2.2)\\
&= \frac{\mathrm{d}x^\alpha}{\mathrm{d}s}\nabla_\alpha \left(K_\beta \frac{\mathrm{d}x^\beta}{\mathrm{d}s}\right) && (2.3)\\
&= \frac{\mathrm{d}x^\alpha}{\mathrm{d}s}\frac{\mathrm{d}x^\beta}{\mathrm{d}s}\nabla_\alpha K_\beta + K_\beta \frac{\mathrm{d}x^\alpha}{\mathrm{d}s}\nabla_\alpha \frac{\mathrm{d}x^\beta}{\mathrm{d}s} && (2.4)\\
&= \frac{\mathrm{d}x^\alpha}{\mathrm{d}s}\frac{\mathrm{d}x^\beta}{\mathrm{d}s}\nabla_{(\alpha} K_{\beta)} + 0 && (2.5)\\
&= 0. && (2.6)
\end{aligned}$$

□

The notion of a Killing vector field has a generalization to tensors for higher rank that satisfy similar properties.

Definition 4. Let $K_{\mu\nu}$ be a symmetric tensor field on a (pseudo)-Riemannian manifold $(M, g_{\mu\nu})$. $K_{\mu\nu}$ is called a **Killing tensor** (field) if

$$\nabla_{(\lambda} K_{\mu\nu)} = 0.$$

There are a number of trivial examples of Killing tensors.

Example 1. For any (pseudo)-Riemannian manifold $(M, g_{\mu\nu})$, the metric tensor itself $g_{\mu\nu}$ is a Killing tensor field.

Example 2. Suppose V^μ and W^μ are Killing vector fields, then $K_{\mu\nu} = V_{(\mu}W_{\nu)}$ is a Killing tensor.

Unlike Killing vectors, Killing tensors do not have an interpretation in terms of spacetime symmetries. Nonetheless, they still lead to constants of motion.

Lemma 3. *Let $x^\mu(s)$ be a geodesic on a (pseudo)-Riemannian manifold $(M, g_{\mu\nu})$, and let $K^{\mu\nu}$ be a Killing tensor field, then the quantity $\mathcal{K} = K_{\mu\nu}\frac{\mathrm{d}x^\mu}{\mathrm{d}s}\frac{\mathrm{d}x^\nu}{\mathrm{d}s}$ is conserved along the geodesic $x^\mu(s)$.*

Proof. Left as an exercise to the reader. □

Example 3. When applied to the metric $g_{\mu\nu}$ this lemma reproduces the familiar result that the norm of the tangent vector to a geodesic $g_{\mu\nu}\frac{\mathrm{d}x^\mu}{\mathrm{d}s}\frac{\mathrm{d}x^\nu}{\mathrm{d}s}$ is preserved along a geodesic.

2.3 Constants of Motion of Kerr geodesics

From the explicit expression for the Kerr metric in Boyer-Lindquist coordinates (1.16), we can immediately infer that the Kerr metric has two Killing vector fields $\left(\frac{\partial}{\partial t}\right)^\mu$ and $\left(\frac{\partial}{\partial \phi}\right)^\mu$, related to the time translation and axial symmetries of the spacetime, respectively. These are all the independent Killing vector fields that the Kerr metric has. (More precisely, all Killing vectors of Kerr can be written as a linear combination of $\left(\frac{\partial}{\partial t}\right)^\mu$ and $\left(\frac{\partial}{\partial \phi}\right)^\mu$).

These Killing symmetries lead to two constants of motion

$$\mathcal{E} = -\left(\frac{\partial}{\partial t}\right)_\alpha \frac{\mathrm{d}x^\alpha}{\mathrm{d}s} = -g_{t\alpha}\frac{\mathrm{d}x^\alpha}{\mathrm{d}s}, \tag{2.7}$$

$$\mathcal{L} = \left(\frac{\partial}{\partial \phi}\right)_\alpha \frac{\mathrm{d}x^\alpha}{\mathrm{d}s} \quad = g_{\phi\alpha}\frac{\mathrm{d}x^\alpha}{\mathrm{d}s}. \tag{2.8}$$

When the affine parameter s is chosen such that $\frac{\mathrm{d}x^\mu}{\mathrm{d}s}$ equals the four momentum p^μ of the particle following the geodesic, $\mathcal{E}$ is equal to the energy of the particle and $\mathcal{L}$ is equal to the component of the orbital angular momentum along the symmetry axis of the Kerr geometry. By analogy, we will refer to $\mathcal{E}$ and $\mathcal{L}$ as the **energy** and **angular momentum** regardless of the chosen affine parameter.

As for any spacetime the metric $g_{\mu\nu}$ is a Killing tensor leading to our third constant of motion, the invariant mass squared

$$\mu = -g_{\mu\nu}\frac{\mathrm{d}x^\mu}{\mathrm{d}s}\frac{\mathrm{d}x^\nu}{\mathrm{d}s}. \tag{2.9}$$

It turns out that Kerr spacetime has an additional "hidden" symmetry in the form of a Killing tensor. This Killing tensor is given by

$$K_{\mu\nu} = \Sigma\left(\ell_\mu n_\nu + \ell_\nu n_\mu\right) + r^2 g_{\mu\nu}, \tag{2.10}$$

where ℓ^μ and n^ν are principal null vectors[3] of the Kerr geometry. In Boyer-Lindquist coordinates their components can be written,

$$\ell^\mu = \left(\frac{r^2+a^2}{\Delta}, 1, 0, \frac{a}{\Delta}\right), \quad \text{and} \tag{2.11}$$

$$n^\mu = \left(\frac{r^2+a^2}{2\Sigma}, -\frac{\Delta}{2\Sigma}, 0, \frac{a}{2\Sigma}\right). \tag{2.12}$$

This gives rise to a fourth constant of motion, the **Carter constant**

$$\mathcal{K} = K_{\mu\nu}\frac{\mathrm{d}x^\mu}{\mathrm{d}s}\frac{\mathrm{d}x^\nu}{\mathrm{d}s}. \tag{2.13}$$

This constant of motion has the rough interpretation as the "total angular momentum squared" of the particle.

Any functional combination of constants of motion is also a constant of motion. It is conventional to use this freedom to replace $\mathcal{K}$ with the constant

$$\mathcal{Q} = \mathcal{K} - \left(\mathcal{L} - a\mathcal{E}\right)^2, \tag{2.14}$$

which (somewhat confusingly) is also referred to as "the Carter constant". (We will be following this tradition.)

[3]This means that they are null vectors k^μ, which satisfy $k^\alpha k^\beta k_{[\mu} C_{\nu]\alpha\beta[\lambda} k_{\rho]} = 0$, which expresses that k^μ is an eigenvector of the Weyl curvature tensor $C_{\mu\nu\rho\sigma}$ in some suitable sense.

2.4 Separating the geodesic equations

So with constants of motion $(\mu, \mathcal{E}, \mathcal{L}, \mathcal{Q})$ in hand, we have four equations that a geodesic must satisfy

$$\mu = g_{\alpha\beta}\frac{\mathrm{d}x^\alpha}{\mathrm{d}s}\frac{\mathrm{d}x^\beta}{\mathrm{d}s}, \tag{2.15}$$

$$\mathcal{Q} + (\mathcal{L} - a\mathcal{E})^2 = K_{\alpha\beta}\frac{\mathrm{d}x^\alpha}{\mathrm{d}s}\frac{\mathrm{d}x^\beta}{\mathrm{d}s}, \tag{2.16}$$

$$\mathcal{E} = -g_{t\alpha}\frac{\mathrm{d}x^\alpha}{\mathrm{d}s}, \tag{2.17}$$

$$\mathcal{L} = g_{\phi\alpha}\frac{\mathrm{d}x^\alpha}{\mathrm{d}s}. \tag{2.18}$$

So, if we fix values of $(\mu, \mathcal{E}, \mathcal{L}, \mathcal{Q})$, we have four equations for four unknowns (the components of $\frac{\mathrm{d}x^\mu}{\mathrm{d}s}$), and we can solve these equations. After some straightforward (but tedious) algebra we find

$$\left(\frac{\mathrm{d}r}{\mathrm{d}s}\right)^2 = \frac{\left(\mathcal{E}(r^2+a^2) - a\mathcal{L}\right)^2 - \Delta\left(\mathcal{Q} + (\mathcal{L}-a\mathcal{E})^2 + \mu r^2\right)}{\Sigma^2} \tag{2.19}$$

$$\left(\frac{\mathrm{d}\cos\theta}{\mathrm{d}s}\right)^2 = \frac{\mathcal{Q} - \cos^2\theta\Big(a^2(\mu - \mathcal{E}^2)\sin^2\theta + \mathcal{L}^2 + \mathcal{Q}\Big)}{\Sigma^2} \tag{2.20}$$

$$\frac{\mathrm{d}t}{\mathrm{d}s} = \frac{\frac{r^2+a^2}{\Delta}\big(\mathcal{E}(r^2+a^2) - a\mathcal{L}\big) - a^2\mathcal{E}\sin^2\theta + a\mathcal{L}}{\Sigma}, \text{ and} \tag{2.21}$$

$$\frac{\mathrm{d}\phi}{\mathrm{d}s} = \frac{\frac{a}{\Delta}\left(\mathcal{E}(r^2+a^2) - a\mathcal{L}\right) + \frac{\mathcal{L}}{\sin^2\theta} - a\mathcal{E}}{\Sigma}. \tag{2.22}$$

This is already a huge improvement over the general geodesic equations in that only first order derivatives appear. Moreover, t and ϕ do not appear at all on the right hand side of the equations. If we can manage to solve the equations for r and θ the solutions for t and ϕ can be found by direct integration. Finally, the equations for r and θ appear almost entirely decoupled, apart from the Σ in the denominators the right hand side of the radial (r) equation depends only on r and the polar (θ) equation depends only on θ. Having decoupled equations would be nice since we could then solve each equation independently. To fully decouple the equations we introduce a new time parameter, the **Mino-Carter time** λ defined by

$$\frac{\mathrm{d}\lambda}{\mathrm{d}s} = \frac{1}{\Sigma}. \tag{2.23}$$

With this choice our equations become

$$\begin{aligned}
\left(\frac{\mathrm{d}r}{\mathrm{d}\lambda}\right)^2 &= \big(\mathcal{E}(r^2+a^2) - a\mathcal{L}\big)^2 - \Delta\left(\mathcal{Q} + (\mathcal{L}-a\mathcal{E})^2 + \mu r^2\right) &&= P_r(r) \\
\left(\frac{\mathrm{d}\cos\theta}{\mathrm{d}\lambda}\right)^2 &= \mathcal{Q} - \cos^2\theta\Big(a^2(\mu-\mathcal{E}^2)\sin^2\theta + \mathcal{L}^2 + \mathcal{Q}\Big) &&= P_\theta(\cos\theta) \\
\frac{\mathrm{d}t}{\mathrm{d}\lambda} &= \frac{r^2+a^2}{\Delta}\big(\mathcal{E}(r^2+a^2) - a\mathcal{L}\big) - a^2\mathcal{E}\sin^2\theta + a\mathcal{L} &&= T_r(r) + T_\theta(\cos\theta) \\
\frac{\mathrm{d}\phi}{\mathrm{d}\lambda} &= \frac{a}{\Delta}\left(\mathcal{E}(r^2+a^2) - a\mathcal{L}\right) + \frac{\mathcal{L}}{\sin^2\theta} - a\mathcal{E} &&= \Phi_r(r) + \Phi_\theta(\cos\theta).
\end{aligned}$$

These equations are completely decoupled. Moreover, the right hand side of the t and ϕ equations separate as the sum of something that depends on r with something that depends on θ. Consequently, these can be integrated separately for different radial and polar solutions.

The equations for r and $\cos\theta$ each individually take the form of a particle moving in a 1-dimensional potential. The functions P_r and P_θ are therefore known as the **radial** and **polar potentials**. Note that instead of the equations involving the square of the first derivatives (for r and θ) we can easily return to second order differential equations (which now will also be decoupled) by taking the derivative with respect to λ to yield

$$\frac{\mathrm{d}^2 r}{\mathrm{d}\lambda^2} = \frac{1}{2}P_r'(r), \quad \text{and} \tag{2.24}$$

$$\frac{\mathrm{d}^2\cos\theta}{\mathrm{d}\lambda^2} = \frac{1}{2}P_\theta'(\cos\theta). \tag{2.25}$$

2.5 The polar equation

$$\left(\frac{\mathrm{d}\cos\theta}{\mathrm{d}\lambda}\right)^2 = \mathcal{Q} - \cos^2\theta\Big(a^2(\mu-\mathcal{E}^2)\sin^2\theta + \mathcal{L}^2 + \mathcal{Q}\Big) = P_\theta(\cos\theta) \tag{2.26}$$

Because the left-hand side of the equation is a square, we can only find solutions if the right-hand side is not negative, i.e. when $P_\theta(\cos\theta) \geq 0$. We can therefore learn about the possible solutions by studying the roots of the polynomial $P_\theta(z)$. Since $P_\theta(z)$ is a fourth order polynomial in $z = \cos\theta$, there at most 4 real roots. Moreover, since $P_\theta(z)$ is an even function of z these roots come in pairs $z = \pm z_i$. Consequently,

$$P_\theta(z) = a^2(\mu-\mathcal{E}^2)(z^2 - z_1^2)(z^2 - z_2^2). \tag{2.27}$$

If we evaluate $P_\theta(z)$ at the poles $z = \pm 1$, we find that $P_\theta(\pm 1) = -\mathcal{L}^2$. We thus immediately learn geodesics can only reach the poles when $\mathcal{L} = 0$.

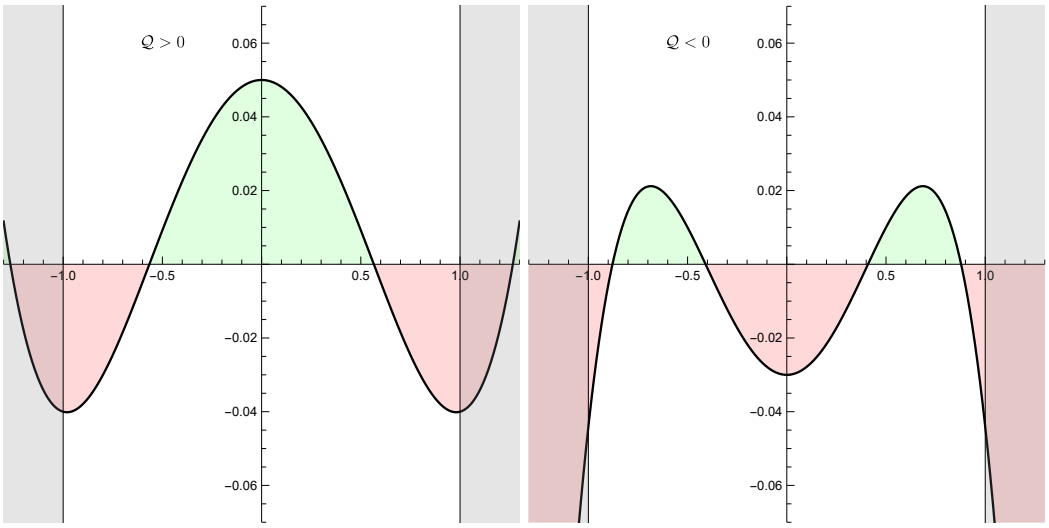

Figure 2.1: The polar potential P_θ when $\mathcal{Q}$ is positive (on the left) or negative (on the right). In the positive $\mathcal{Q}$ case, we find solutions where $\cos\theta$ oscillates around the equator ($\cos\theta = 0$) between $\pm z_1$. In the negative $\mathcal{Q}$ case, we can get vortical solutions where $\cos\theta$ oscillates between $z_1 < z_2$ (or $-z_2 < -z_1$), but never crosses the equator.

When we evaluate $P_\theta(z)$ on the equator $\cos\theta = 0$ we find that $P_\theta(0) = \mathcal{Q}$. Therefore, we only find solutions that visit the equator when $\mathcal{Q} \geq 0$. If $\mathcal{Q} > 0$ and $\mathcal{L} \neq 0$, there must be an odd number of zeroes between 0 and 1, and the same number between -1 and 0. Since there are at most 4 zeroes, there is exactly one such zero z_1, and the only solutions oscillate around the equator between $\pm z_1$. In the Schwarzschild ($a \to 0$) limit, these solutions describe trajectories whose orbital plane is inclined relative to the equator of the coordinate system. As such these solutions are generally known as **inclined** trajectories. In Kerr this orbital plane precesses, leading to another common name **precessing** trajectories.

If $\mathcal{Q} = 0$, then $z = 0$ is a double root of P_θ. This implies that $x = \cos\theta = 0$ is constant is a solution to the differential equation. These solutions stay in the Kerr equatorial plane and are therefore known as **equatorial** trajectories.

If $\mathcal{Q} < 0$ then no solution is possible near the equator. In this case, it is only possible for P_θ to be positive somewhere in the range $-1 < \cos\theta < 1$, if P_θ has exactly two zeroes $0 < z_1 < z_2 \leq 1$. We can easily see that this is only possible if $\mu < \mathcal{E}^2$ by considering the behavior of P_θ at large z. At large z, $P_\theta = a^2(\mu - \mathcal{E}^2)z^4 + \mathcal{O}(z^2)$. So, if $\mu > \mathcal{E}^2$ the polar potential becomes positive at large z. Consequently, there must be at least one zero between $z = 1$ (where P_θ is negative) and $z = \infty$, and there cannot be four roots in

Type	$\mu - \mathcal{E}^2$	$\frac{\mathcal{L}^2}{a^2(\mathcal{E}^2-\mu)}$	$\mathcal{Q}$	$z = \cos\theta$
Equatorial	any	any	0	0
Inclined	any	any	> 0	$-z_1 < z < z_1$
Vortical	< 0	≤ 1	$-1 \leq \frac{\mathcal{Q}}{\left(\lvert\mathcal{L}\rvert - \lvert a\rvert\sqrt{\mathcal{E}^2-\mu}\right)^2} \leq 0$	$z_1 < \lvert z\rvert < z_2$

Table 2.1: Classification of solutions of the polar equation.

the range $-1 < z < 1$. The condition $\mu < \mathcal{E}^2$ is by itself not sufficient the existence of two zeroes $0 < z_1 < z_2 \leq 1$. One can show (but we will not here) that such roots exist if and only if the following conditions are met

$$\mathcal{L}^2 \leq a^2(\mathcal{E}^2 - \mu) \text{ and } -\left(|\mathcal{L}| - |a|\sqrt{\mathcal{E}^2 - \mu}\right)^2 \leq \mathcal{Q} \leq 0. \tag{2.28}$$

Solutions of this type are referred to as **vortical** trajectories.

2.6 The radial equation

The decoupled equation for radial motion is given by

$$\left(\frac{\mathrm{d}r}{\mathrm{d}\lambda}\right)^2 = \left(\mathcal{E}(r^2 + a^2) - a\mathcal{L}\right)^2 - \Delta\left(\mathcal{Q} + (\mathcal{L} - a\mathcal{E})^2 + \mu r^2\right) = P_r(r). \tag{2.29}$$

It has the same, overall structure as the polar equation. In particular, we can only have solutions when the radial potential P_r is non-negative, and the radial potential is a fourth order polynomial in r, which therefore has four zeroes r_i (0,2, or 4 of which may be real-valued) and can be written

$$P_r = (\mathcal{E}^2 - \mu)(r - r_1)(r - r_2)(r - r_3)(r - r_4). \tag{2.30}$$

As with the polar equation it will be useful to examine the value of P_r at specific values of r. We start with $r = 0$, and observe that $P_r(0) = -a^2\mathcal{Q}$. Consequently, solutions to the radial equation can only reach $r = 0$ if $\mathcal{Q} \leq 0$, i.e. only equatorial and vortical trajectories can ever reach $r = 0$. Of these, only the equatorial ($\mathcal{Q} = 0$) solutions can ever reach the curvature singularity at $\theta = \pi/2$. We thus find that of all geodesics in Kerr only a measure zero subset hit the singularity. All others miss it entirely, some of them passing through the ring singularity to the $r < 0$ region (all of them vortical) and some of them scattering back due to centrifugal barrier.

Next we turn our attention to the horizon $r_\pm$, since Δ vanishes here we find

$$P_r = \left(\mathcal{E}(r_\pm^2 + a^2) - a\mathcal{L}\right)^2 \geq 0. \tag{2.31}$$

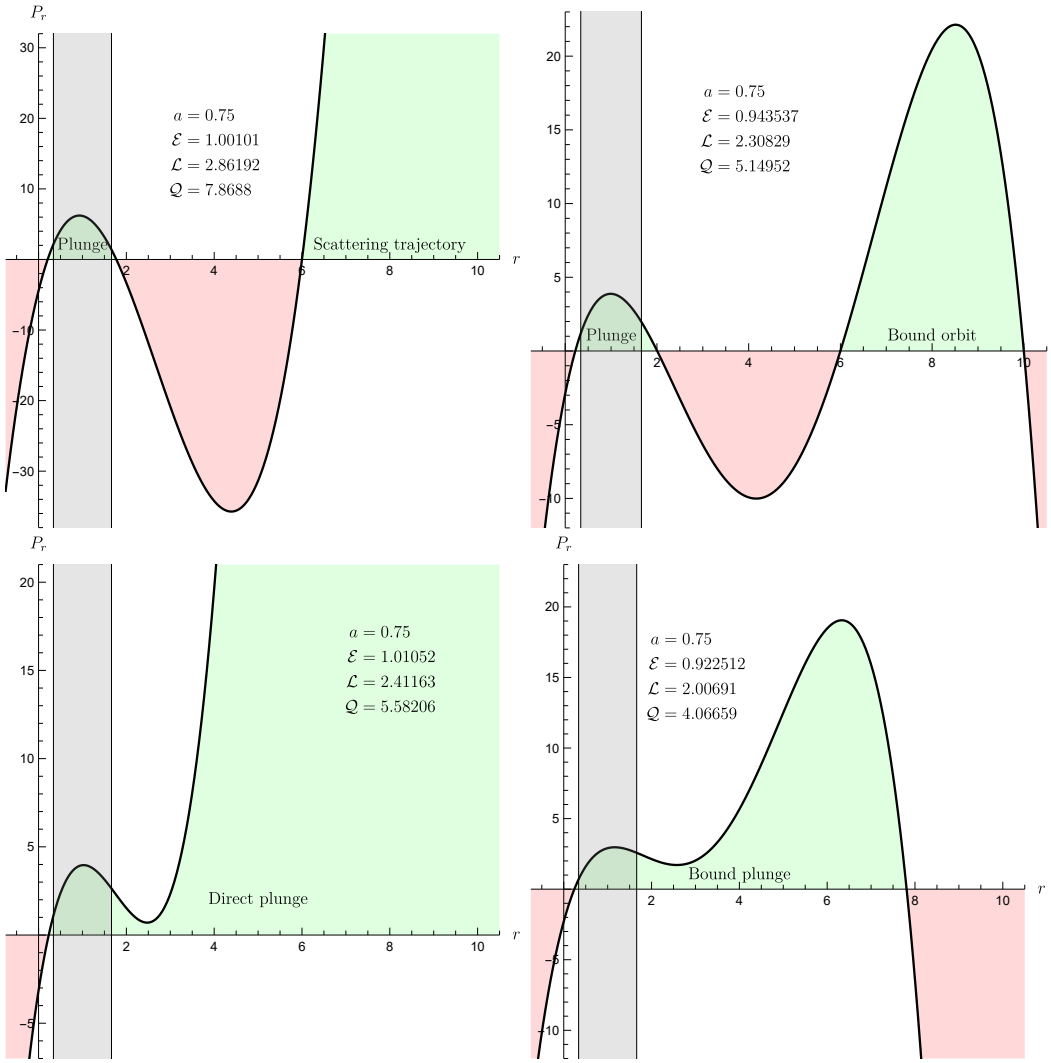

Figure 2.2: The radial potential P_r for a scattering trajectory (top left), bound orbit (top right), direct plunge (bottom left), and bound plunge (bottom left). Note the existence of secondary "deeply bound" plunge solutions in the top plots.

Consequently, for all values of $(\mu, \mathcal{E}, \mathcal{L}, \mathcal{Q})$ that allow the existence of solutions to the polar equation, we have solutions that cross the horizons. Moreover, since r is timelike between the horizons, we cannot have any zeroes between $r_\pm$ for timelike $\mu > 0$ and null $\mu = 0$ solutions. This also implies that if $\mathcal{Q} > 0$ then there must exist at least one (and at most three) zeroes between the inner horizon r_- and $r = 0$.

Last we turn our attention to the behavior of P_r as r approaches $\pm\infty$. Expand P_r we find $P_r = (\mathcal{E}^2 - \mu)r^4 + \mathcal{O}(r^3)$. Consequently, in order for a geodesic to reach infinity $(\mathcal{I}^\pm, i^\pm, i^0)$ it must have $\mathcal{E}^2 > \mu$. For this reason geodesics satisfying this condition are referred to as **unbound**. Note that for null geodesics $\mu = 0$; they are necessarily unbound.

For unbound $\mathcal{E}^2 > \mu$ geodesics the radial potential must have an even number of zeroes between the outer horizon r_+ and $r = \infty$. When there no zeroes in this region the solution corresponds to a trajectory that starts at infinity and dives directly into the black hole. These solutions are known as **direct plunges**.

If there are two zeroes $r_1 > r_2$ in the region outside of the black hole, solutions correspond to trajectories starting from infinity, and scattering of the black hole potential back to infinity. This trajectories are known as **scattering** or **hyperbolic** trajectories.

Geodesics with $\mathcal{E}^2 < \mu$ are only possible for timelike trajectories with $\mu > 0$, and known as **bound** trajectories because they do not possess enough energy to reach infinity. The existence of a polar solution implies that for bound orbits we necessarily have that $\mathcal{Q} \geq 0$, and therefore that there exists at least one zero inside the inner horizon. Since the radial potential changes sign between the outer horizon r_+ and infinity there must be either one or three zeroes outside the outer horizon.

If there exists just one zero $r_+ < r_1 < \infty$ the solution corresponds to a trajectory starting at the past horizon moving outward to r_1 and then diving back into the black hole. These trajectories are known as **(bound) plunges**. Of course, these geodesics do not stop at the horizon. If followed into the black hole, they will also cross the inner horizon before encountering a turning point in the inner region, and proceeding back outward through the inner horizon and exiting the outer horizon into a new parallel universe in the maximally extended Kerr solution, after which the above repeats ad infinitum with the geodesic eventually (according to its own proper time) visiting infinitely many copies of the external universe.

If there are three zeroes $r_+ < r_3 < r_2 < r_1 < \infty$ then the solution oscillates between r_1 and r_2 to form a **bound (eccentric) orbit**.

Note that both in the case of bound orbits and scattering orbits, there exists a secondary solution with the same constants of motion which oscillates

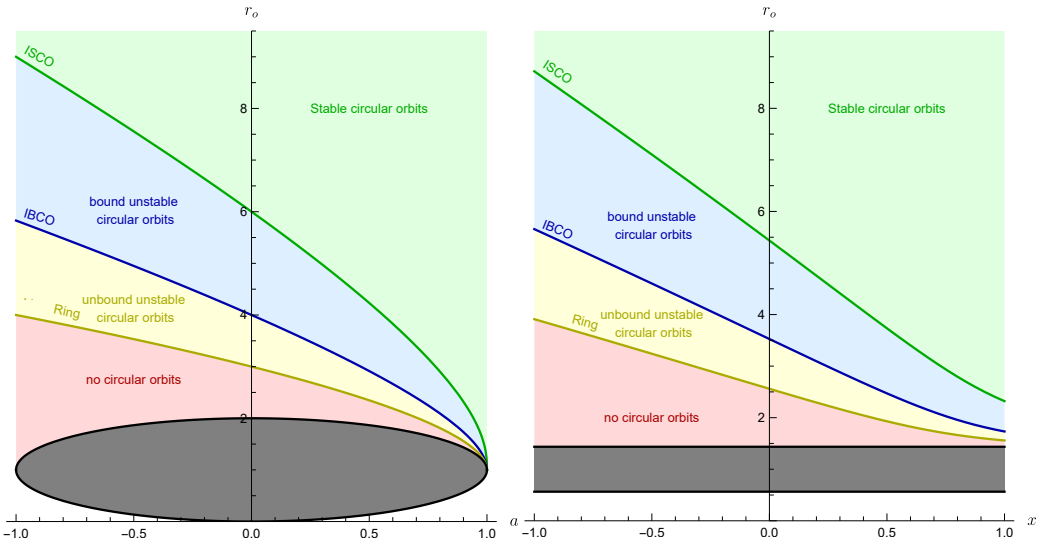

Figure 2.3: The location of the ISCO, IBCO, and light ring in Kerr. On the left, equatorial orbits, on the right at fixed spin $a = 0.9M$.

between the remaining turning point outside the horizon and the zero inside the inner horizon (if $\mathcal{Q} > 0$). These solutions behave similarly to the bound plunges and are therefore known as **deeply bound plunges**.

2.6.1 Circular orbits

Circular orbits are geodesics for which the radial potential allows a constant solution r_o. This requires not only that $P_r(r_o) = 0$ (which ensures that $\frac{\mathrm{d}r}{\mathrm{d}\lambda} = 0 = \frac{\mathrm{d}r}{\mathrm{d}s}$), but also that $P_r'(r_o) = 0$ (which ensures that $\frac{\mathrm{d}^2r}{\mathrm{d}\lambda^2} = 0 = \frac{\mathrm{d}^2r}{\mathrm{d}s^2}$). This therefore requires that r_o is a double zero of the radial potential. A double zero can be either a maximum or minimum of the radial potential. In the former case the circular orbit is **stable**; any small perturbation will produce an eccentric orbit with small eccentricity. In the later case, the circular orbit is **unstable**; any perturbation leads to a wildly different orbit.

Stable circular orbits occur as the limit of eccentric orbits as the zeroes r_1 and r_2 merge. Unstable circular orbits are formed by merging the inner turning point of a scattering or bound orbit with the outer turning point of a deeply bound plunge.

Stable circular orbits can only be found outside a certain radius, the **innermost stable circular orbit** or **ISCO**. Inside this radius one can still find circular orbits, but the become increasingly unstable with larger and larger energies. Initially, these unstable circular orbits have low enough

energies, that even after a perturbation the particle will stay bound to the black hole. However, below another radius, the **innermost bound circular orbit** or **IBCO**, the energy becomes large enough that perturbations can send the particle scattering to infinity. Finally, the energy of the circular orbits diverges at the **light ring**, this radius can only be approached if one simultaneously allows the mass μ to go to zero, and the geodesic to become null. Inside the light ring no circular orbits are possible (outside the event horizon).

2.7 Characterizing bound orbits

In the previous sections we have found the bound orbits ($\mu > \mathcal{E}^2$) are necessarily either inclined ($\mathcal{Q} > 0$) or equatorial ($\mathcal{Q} = 0$), and corresponds a solution oscillating in the radial direction between $r_1 \geq r_2 > r_+$, and in the polar direction between $\pm z_1$. There are a number of characterizations of these orbits that useful in identifying them

- The **constants of motion** $(\mathcal{E}, \mathcal{L}, \mathcal{Q})$. For any sets of values of the constants of motion, if a bound orbit exists then that solution is unique. (There will always also exist a deeply bound plunge with the same constants of motion.)

- The **turning points** (r_1, r_2, z_1) uniquely characterize a bound orbit up to the direction of motion: with the rotation of the black hole (**prograde**) or against the rotation of the black hole (**retrograde**). This degeneracy is conventionally broken by the convention that the angular momentum $\mathcal{L}$ is always positive, and letting the sign of the spin determine the sense of the motion. The turning point r_1 is known as the **apocenter** and r_2 as the **pericenter**.

- A Keplerian-like parametrization consting of the

$$p = \frac{2r_1 r_2}{r_1 + r_2} \qquad \textbf{semi-latus rectum}$$

$$e = \frac{r_1 - r_2}{r_1 + r_2} \qquad \textbf{eccentricity}$$

$$x = \begin{cases} \sqrt{1 - z_1^2} & \text{prograde} \\ -\sqrt{1 - z_1^2} & \text{retrograde} \end{cases} \qquad \textbf{inclination}$$

  In this parametrization $e = 0$ corresponds to circular motion, and $x = \pm 1$ corresponds to equatorial motion.

- A more phenomenological characterization is in terms of **periods** of orbit
  - Λ_r The (Mino time) period of the radial motion.
  - Λ_θ The (Mino time) period of the polar motion.
  - Λ_ϕ The average Mino time needed to complete an orbital cycle.

  The triple $(\Lambda_r, \Lambda_\theta, \Lambda_\phi)$, uniquely identifies a (relativistic) bound orbit. This may come as surprise to those familiar of Newtonian orbital dynamics where we always have $\Lambda_r = \Lambda_\theta = \Lambda_\phi$.

- Similarly, the **Mino time frequencies**

$$\begin{aligned}
\Upsilon_r &= \frac{2\pi}{\Lambda_r} \\
\Upsilon_\theta &= \frac{2\pi}{\Lambda_\theta} \\
\Upsilon_\phi &= \frac{2\pi}{\Lambda_\phi} = \lim_{\Lambda\to\infty} \frac{1}{2\Lambda} \int_{-\Lambda}^{\Lambda} \frac{\mathrm{d}\phi}{\mathrm{d}\lambda}\,\mathrm{d}\lambda.
\end{aligned}$$

In the same spirit as the azimuthal frequency we can define the average advance of the Boyer-Lindquist time t,

$$\Upsilon_t = \lim_{\Lambda\to\infty} \frac{1}{2\Lambda} \int_{-\Lambda}^{\Lambda} \frac{\mathrm{d}t}{\mathrm{d}\lambda}\,\mathrm{d}\lambda.$$

This allows us to define the **Boyer-Lindquist frequencies** of the orbit.

$$\begin{aligned}
\Omega_r &= \frac{\Upsilon_r}{\Upsilon_t} \\
\Omega_\theta &= \frac{\Upsilon_\theta}{\Upsilon_t} \\
\Omega_\phi &= \frac{\Upsilon_\phi}{\Upsilon_t}.
\end{aligned}$$

The Boyer-Lindquist frequencies are frequencies that a distant observer at rest would infer when observing the system. Unlike the Mino-time frequencies the triple $(\Omega_r, \Omega_\theta, \Omega_\theta)$ does not always uniquely identify a bound orbit. In the strong field regime, we typically encounter pairs of distinct **isofrequency** orbits with the same Boyer-Lindquist frequencies.

Two other commonly observed quantities are :

- The **pericenter advance** $\Upsilon_\phi \Lambda_r - 2\pi$

- The **nodal advance** $\Upsilon_\phi \Lambda_\theta - 2\pi$

Although we are not going to derive them here, explicit expressions for all these quantities (and the corresponding geodesic solutions) can be obtained analytically by solving the ODEs. These solutions can be obtained e.g. from the Black Hole Perturbation Toolkit [1].

2.8 Null geodesics and black hole shadows

Null geodesics describe the trajectories of light rays through the spacetime. From the analysis in the previous sections we note that setting $\mu = 0$ implies that null geodesics are always unbound. As observers far away from a typical black hole we are interested in light rays that can reach as at infinity. We found that there is two main possibilities if we follow such a ray back in time either:

- The ray follows a scattering trajectory with $r \geq r_2 \geq r_3 > r_+$. In this case the polar motion must be either equatorial or inclined.

  or

- The ray follows a (time reversed) direct plunge originating from the past horizon (with no zeroes outside the horizon). In this case the polar motion can be any of equatorial, inclined, or vortical.

More coming...

Bibliography

[1] Black Hole Perturbation Toolkit. (bhptoolkit.org).

[2] Robert H. Boyer and Richard W. Lindquist. Maximal analytic extension of the Kerr metric. **J. Math. Phys.**, 8:265, 1967.